RESEARCH PAPER

CrossMark

Mechanical behavior of composite parts adhesively jointed with the insert double-lap joint under tensile load

İsmail Yasin Sülü [1]

Abstract

In this paper, composite parts jointed with insert double-lap joint (DLJ) subjected to tensile load were analyzed by using 3-D finite element method (FEM). In the analysis, the composite parts were carbon/epoxy (T 700) with different fiber orientation angles and the adhesive was DP 410. The models for the numerical analyses were generated by using the ANSYS 14.5 software package. The finite element analyses (FEA) were carried out to predict the failure loads. Stress at x, y, and z directions; shear stresses; and the von-Mises stresses on adhesive were obtained at the time of the failure for predetermined parameters. Consequently, the effects of orientation angles, overlap widths and length, and adhesive layer were examined. The most effective parameters were determined for composite parts adhesively bonded with the double lap joint.

Keywords Joint design · Stress analysis · Composite · Finite element analysis · Non-linear analysis · Adhesive joint

1 Introduction

The classical single lap and double lap joints are preferred in both bonding and repair of damaged parts in aerospace, machine design, automotive, and a lot of industry areas. These joints technique is widely used for metal and composite parts. Similarly, the use of adhesives and composite parts in the industry are increasing because of their ease of application, high strength, and various other properties. It is important to the formation of strong joints by the use of adhesives while bonding composite parts. Also, it is important not to be taking up much space. Therefore, a lot of studies have been made about the joining of composite parts.

The mechanical behavior of composite parts is among the most important factors in determining the work life of composite parts. That is why, bonding and repair methods are important for composites and a lot of materials. Hence, many studies have been carried out in literature for single-lap and double-lap adhesive joints of composite parts, their joining regions, and the mechanical behavior of adhesive joints of composite parts under different loads and parameters. It is important that composite parts are generally joined by adhesive bonding methods with high joint efficiency. Therefore, the failure prediction of the composite-composite and composite-steel single-lap joints with adhesive bondline was investigated [1–11]. Also, there are a lot of double lap joints studies in literature. Tsai and Morton investigated experimentally [12] the mechanics of double-lap joints with unidirectional ($[0°]_{16}$) and quasi-isotropic ($[0°/90°/-45°/45°]_{2S}$) composite adherents under tensile loading, numerically with a finite element method, and analytically through a one-dimensional closed-form solution. A linear-elastic two-dimensional finite element model was developed for comparison with the experimental results and to provide deformation and stress distributions for the joints. In another study, Marannano and Zuccarello carried out [13] contribution to the knowledge of the mechanical behavior of hybrid bonded/riveted joints, in the present work a numerical–experimental study of bonded/riveted double-lap joints

✉ İsmail Yasin Sülü
  ismail.sulu@inonu.edu.tr

[1] Department of Mechanical Engineering, Inonu University, Malatya, Turkey
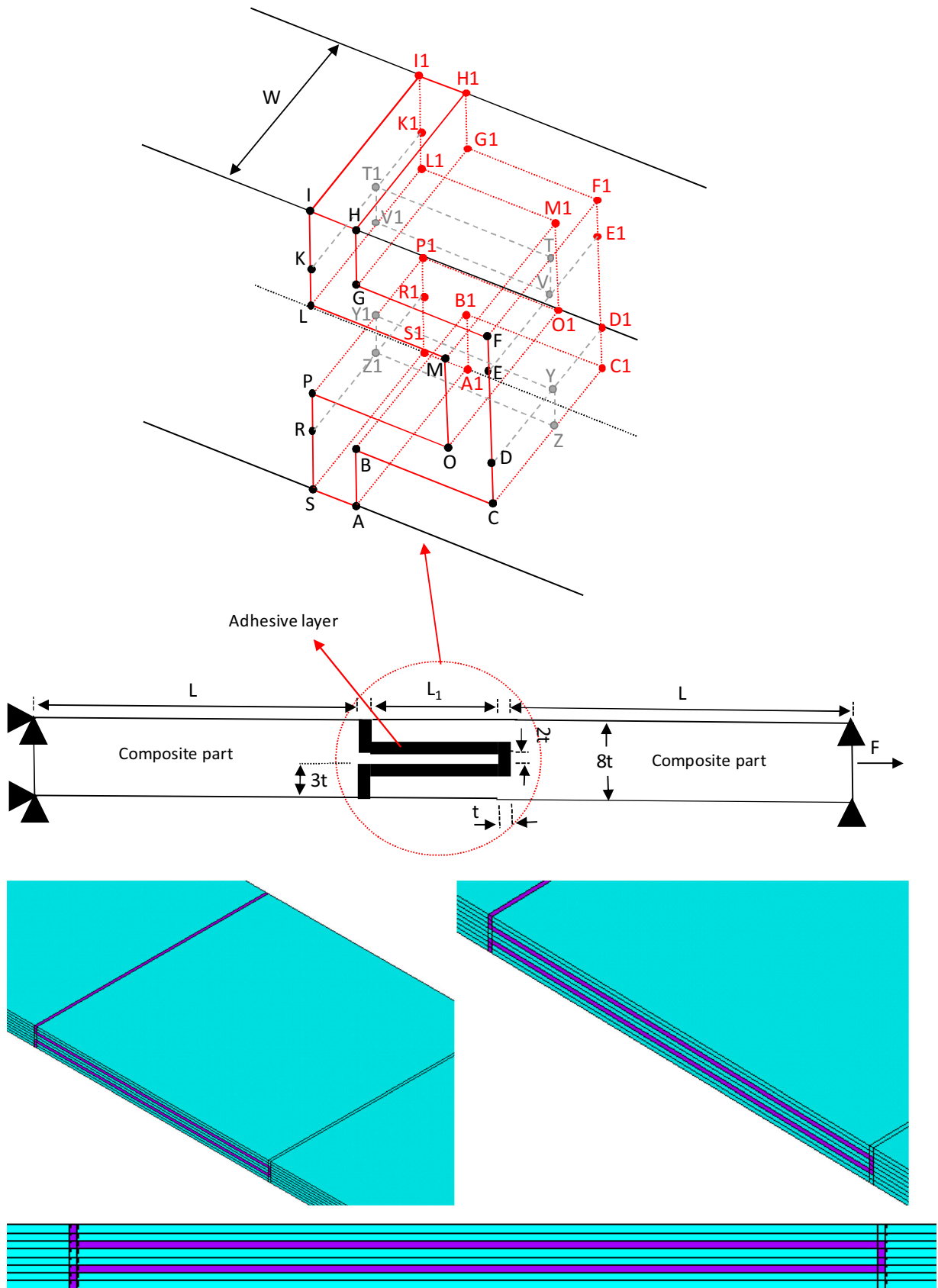
Fig. 1 Composite parts jointed with insert joint subjected to tensile load

Table 1 Material constants for T 700 carbon/epoxy [22]

Properties	Carbon/epoxy (T 700)
E_x (MPa)	132000
E_y (MPa)	10300
E_z (MPa)	10300
G_{xy} (MPa)	6500
G_{yz} (MPa)	3910
G_{xz} (MPa)	6500
ν_{xy}	0.25
ν_{yz}	0.38
ν_{xz}	0.25
X_T (MPa)	2100
Y_T (MPa)	24
Z_T (MPa)	24
X_C (MPa)	1050
Y_C (MPa)	132
Z_C (MPa)	132
S_{xy}(MPa)	75
S_{yz}(MPa)	75
S_{xz}(MPa)	75

Table 3 Orientation angles used in the studies

	Orientation angles (°)
Type A	$[0°/0°/0°/0°]_s$
Type B	$[15°/-15°/15°/-15°]_s$
Type C	$[30°/-30°/30°/-30°]_s$
Type D	$[45°/-45°/45°/-45°]_s$
Type E	$[60°/-60°/60°/-60°]_s$
Type F	$[75°/-75°/75°/-75°]_s$
Type G	$[90°/90°/90°/90°]_s$

determined for different orientation angles and different over-lap widths and lengths. The orientation angles were an effective parameter for mechanical behavior of composites. Hence, orientation angles were considered. Composite parts with the insert double-lap adhesive joint subjected to tensile load were investigated via non-linear FEA. Stress at x, y, and z directions; shear stresses; and the von-Mises stresses on adhesive were obtained at the time of the failure for predetermined parameters. Both the objective of this study was to put forth the many advantages of composites parts and a lot of advantages as high strength, more practical, and easy to use for the industrial applications of adhesive. Also, it was to show that there are many advantages of bonding with the insert DLJ.
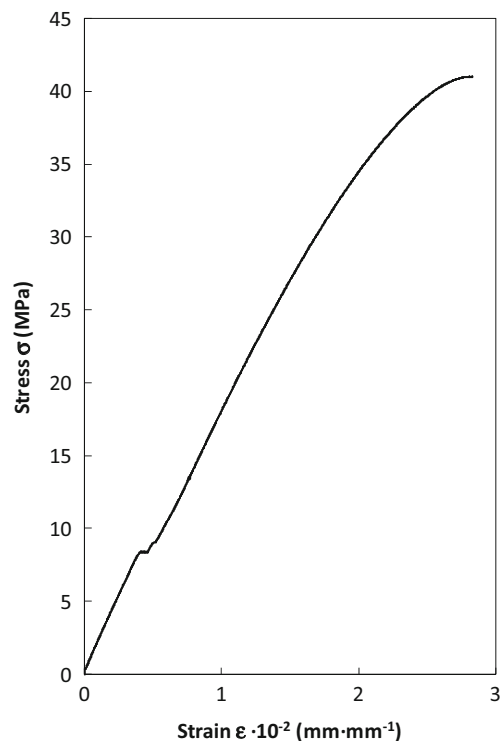
between aluminum and carbon fiber reinforced polymer (CFRP) laminates. Chataigner et al. [14] provided for a civil engineering application a simple design tool of bonded anchorages. More consistent results were obtained concerning the anchorage length and a failure criterion could be expressed in terms of a maximum yielded length along the bonded joint. The validity of this criterion was assessed via an experimental investigation which includes material characterization as well as double lap joints quasi-static loading. Moreover, Goglio and Rossetto [15] noticed that the analytical solutions reproduce in general terms the stress field. They focused the attention on the double lap joint. The performance of a one-dimensional solution for the double lap joint—accounting for bending of the gussets—was compared to the corresponding Volkersen's solution and to finite element results. Additionally, there are several studies about double lap joint [16–20].

In this study, composite parts with different orientation angle and DP 410 type adhesive were used. Studies were carried out numerically. Failure loads were

Table 2 Material constants for DP 410 adhesive [23]

	DP 410 adhesive
Young's modulus E_a(MPa)	2567.45
Poisson's ratio ν_e	0.31
Yield strength σ_y(MPa)	38
Ultimate tensile strength σ_t(MPa)	40.79
Ultimate tensile strain ε_t (mm·mm^{-1})	0.027

Fig. 2 Tensile stress–strain curve of adhesives for DP 410 [23]

**Fig. 3** Mesh details and boundary condition
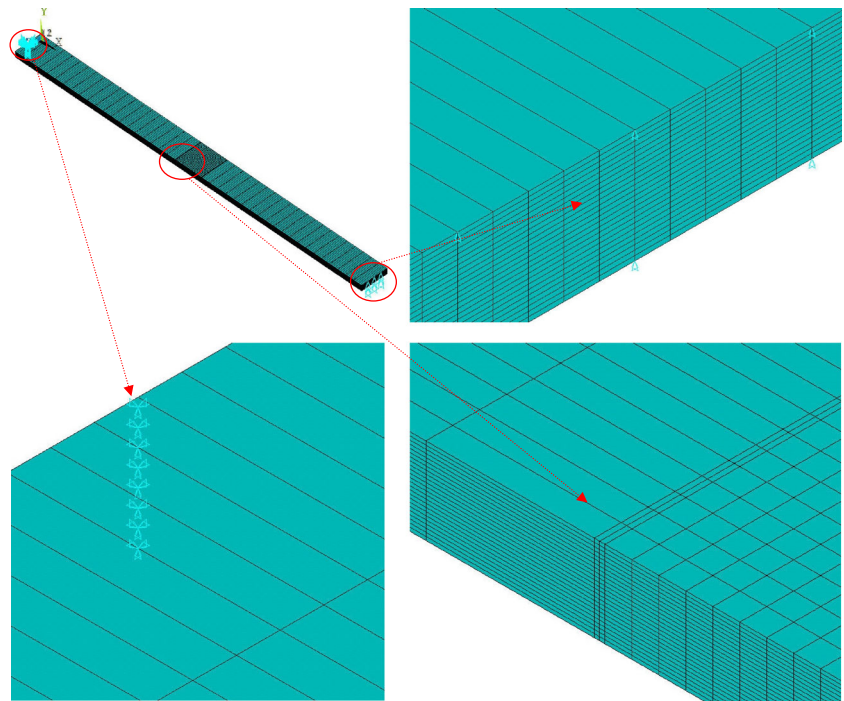
2 3-D non-linear finite element modeling

Composite parts jointed with DLJ subjected to tensile load were shown in Fig. 1. Composite parts were eight layered carbon/epoxy (T 700). In the finite element studies, DP 410 type adhesive was used. The mechanical properties of composite parts and adhesive were shown in Tables 1 and 2, respectively. Different orientation angles shown in Table 3 were used. The true tensile stress-strain behaviors for adhesives were shown in Fig. 2.

The total thicknesses of composite parts with carbon fiber reinforcement were 8×0.2 mm and each layer thickness was 0.2 mm, the thickness of adhesive was

Fig. 4 The von-Mises stress distributions along the upper and below mid-bondlines (shown in Fig. 1: on the adhesive region compared for 15 mm of adherent length and Type A, **a** along the upper and below mid-bondlines and **b** along the both edges
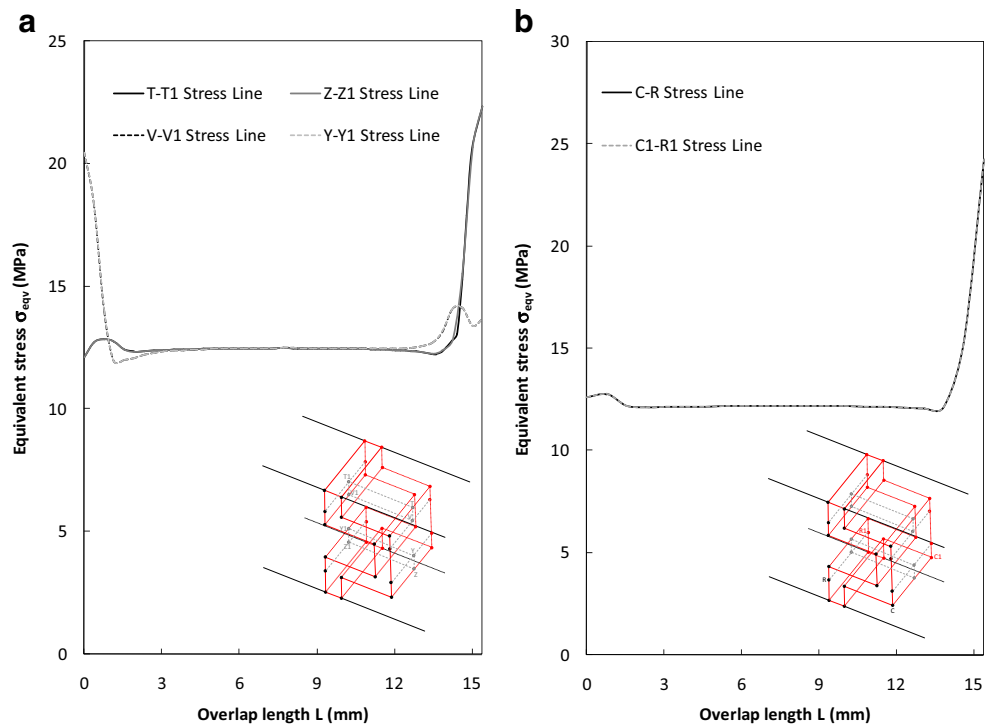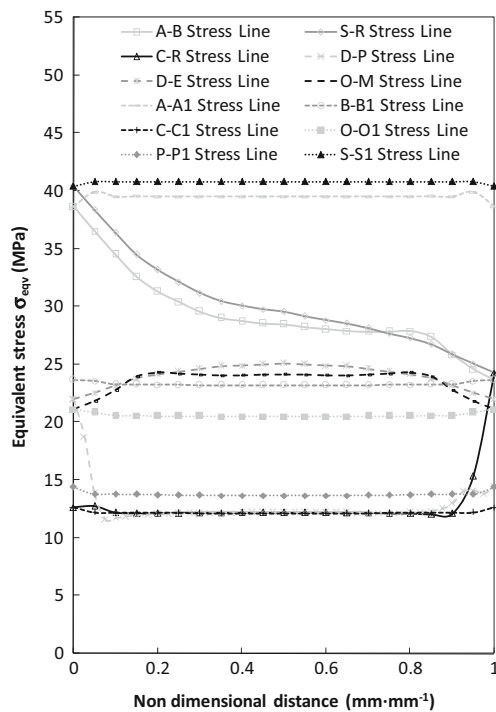
Fig. 5 The von-Mises stress distributions along the different bondlines (shown in Fig. 1: on the adhesive region compared for 15 mm of adherent length and Type A

0.2 mm (t). The length of the composite parts was 62.5 mm (L), overlap-lap lengths were 10, 15, and 20 mm (L_1).

In the finite element studies, composite parts adhesively jointed with insert subjected to tensile load were simulated via the finite elements method. Three dimensional non-linear finite elements model was generated during the analysis of composite parts joined with insert joint. Twenty node isoperimetric quadrangular elements, SOLID186, were used in the macro ANSYS 14.5 version generated for the models. The SOLID186 element is defined with 20 nodes having three degrees of freedom at each node, i.e., translation in the nodal x, y, and z directions. The first end of composite parts joined with double lap joint was fixed in the nodal x, y, and z directions; the other end was only fixed in the nodal y direction. Load was applied in the x direction and load was increased step by step in small values. When a numeric model was created in the ANSYS 14.5 software, the same element type was used to make the adhesive compatible with the composite parts. In order to sensitively obtain the stresses to be investigated, the interface of adhesive and composite parts was densely modeled with meshes. Stress lines were formed on all the surfaces to determine the region where the stresses were high. The joint configuration, boundary conditions, and mesh details considered in this study were represented in Fig. 3. Stress analyses were carried out for composite parts bonded with the insert DLJ subjected to tensile load, and stress distributions for all the layers of the composite parts were calculated by taking into consideration Tsai-wu failure criteria for composites and the von-Mises failure criteria for adhesive [21, 23, 25, 26].

3 Results and discussion

3.1 Effect of orientation angles and overlap on stress distribution

The stress distributions of composite parts bonded with the insert DLJ subjected to tensile load were compared, and the joint with 15 mm overlap length and $[0°/0°/0°/0°]_s$, $[15°/-15°/15°/-15°]_s$, $[30°/-30°/30°/-30°]_s$, $[45°/-45°/45°/-45°]_s$, $[60°/-60°/60°/-60°]_s$, $[75°/-75°/75°/-75°]_s$, and $[90°/90°/90°/90°]_s$ orientation angles were only analyzed. For this, the joint was subjected to tensile load. The orientation angles were important for the mechanical behavior of composite laminates. Several bondlines existed on the adhesive side in the bonding region of the joint with the insert joint (Fig. 1). The von-Mises stress distributions along the upper and below mid-bondlines were compared and stresses on T-T1 and Z-Z1, V-V1, and Y-Y1 stress lines were seen to be of nearly similar stress behavior in Fig. 4a. Also, the von-Mises stress distributions along below edges-bondlines were compared and stresses on C-R and C1-R1 stress lines were seen to be nearly of similar stress behavior in Fig. 4b. The similar stress distributions were nearly observed in these bondlines. Hence, the von-Mises stress distributions along below the adhesive region bondlines were compared and stresses on A-B, S-R, C-R, D-P, D-E, O-M, A-A1, B-B1, C-C1, O-O1, P-P1, and S-S1 stress lines were compared in Fig. 5. The stress lines for the maximum and critical stress region were examined. The Von Mises equivalent stress at the S-S1 bondline was maximum. Also, all failures were on the adhesive region. So, in this study, all stress distributions plotted were for the S-S1 bond-line on the adhesive region.

The stress distributions of the joint under tensile load were given in Figs. 6 to 7. The stresses of the joint with the insert DLJ were generally bigger at the S-S1 line. Stress at x, y, and z directions; shear stresses; and the von-Mises stresses on adhesive were calculated using numerically obtained failure tensile loads. When Figs. 6 to 7 were examined, the stresses that were

Fig. 6 Stress distributions compared for all orientations along S-S1 on the adhesive for 15 mm of adherent length. **a** Stress at x direction. **b** Stress at y direction. **c** Stress at z direction. **d** Equivalent stress σ_{eqv}
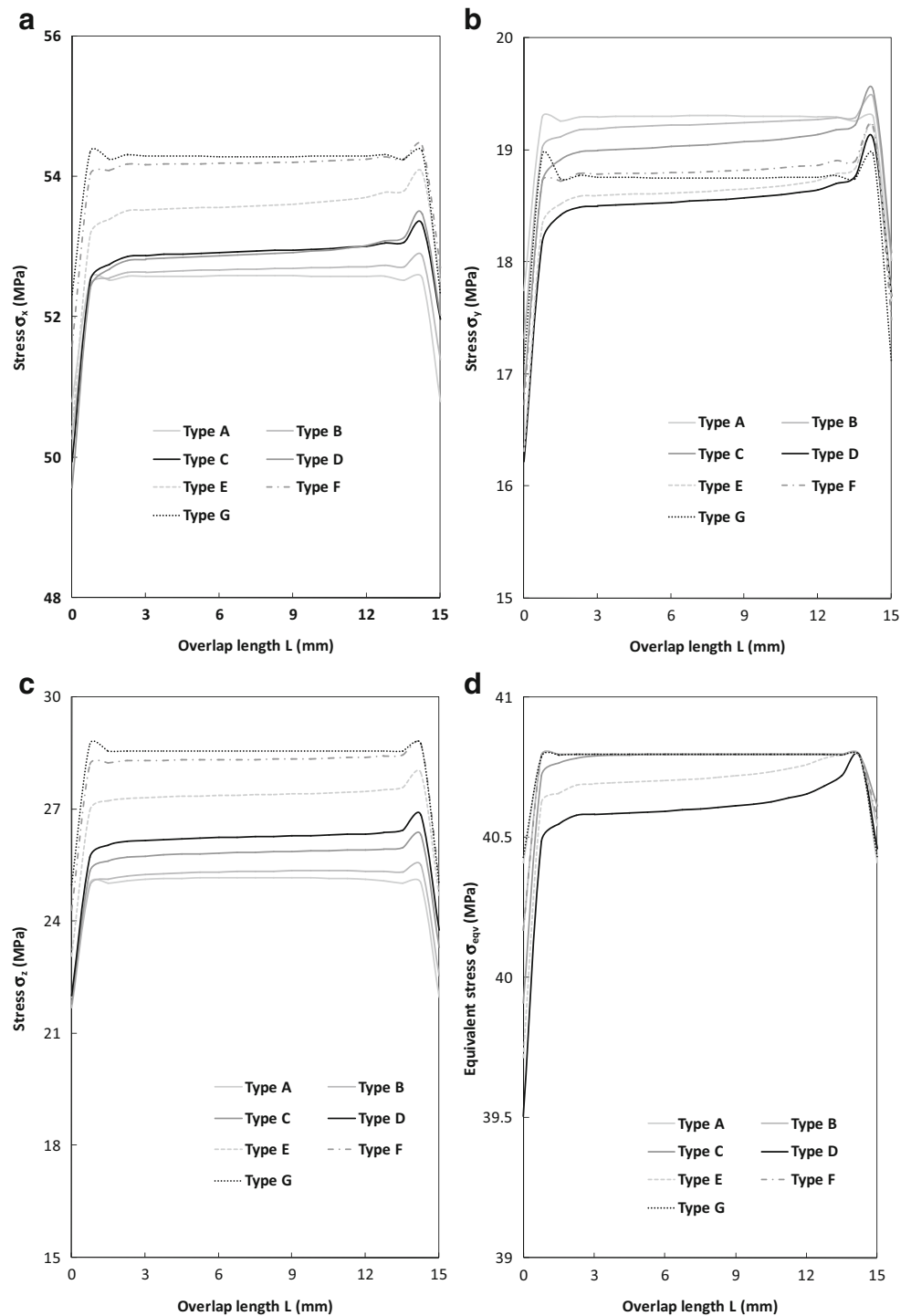
obtained on the adhesives as a result of the joining of composite parts with adhesive could be seen.

The effects of orientation angles on adhesive layers were given in Figs. 6 to 7. It could be seen in the figures that the highest stresses on the adhesive region ends subjected to tensile load were those that occurred in the S-S1 line. In general, it was observed that σ_x and

σ_z on the adhesive layer were maximum when composite parts with $[90°/90°/90°/90°]_s$ orientation angles were jointed. σ_y on the adhesive layer was maximum when composite parts with $[0°/0°/0°/0°]_s$ orientation angles were jointed. The von Mises stress on the adhesive region was minimum when composite parts with $[45°/-45°/45°/-45°]_s$ and $[60°/-60°/60°/-60°]_s$ orientation

Fig. 7 Shear stress distributions compared for all orientations along S-S1 on the adhesive for 15 mm of adherent length, **a** σ_{xy}, **b** σ_{yz}, and **c** σ_{xz}
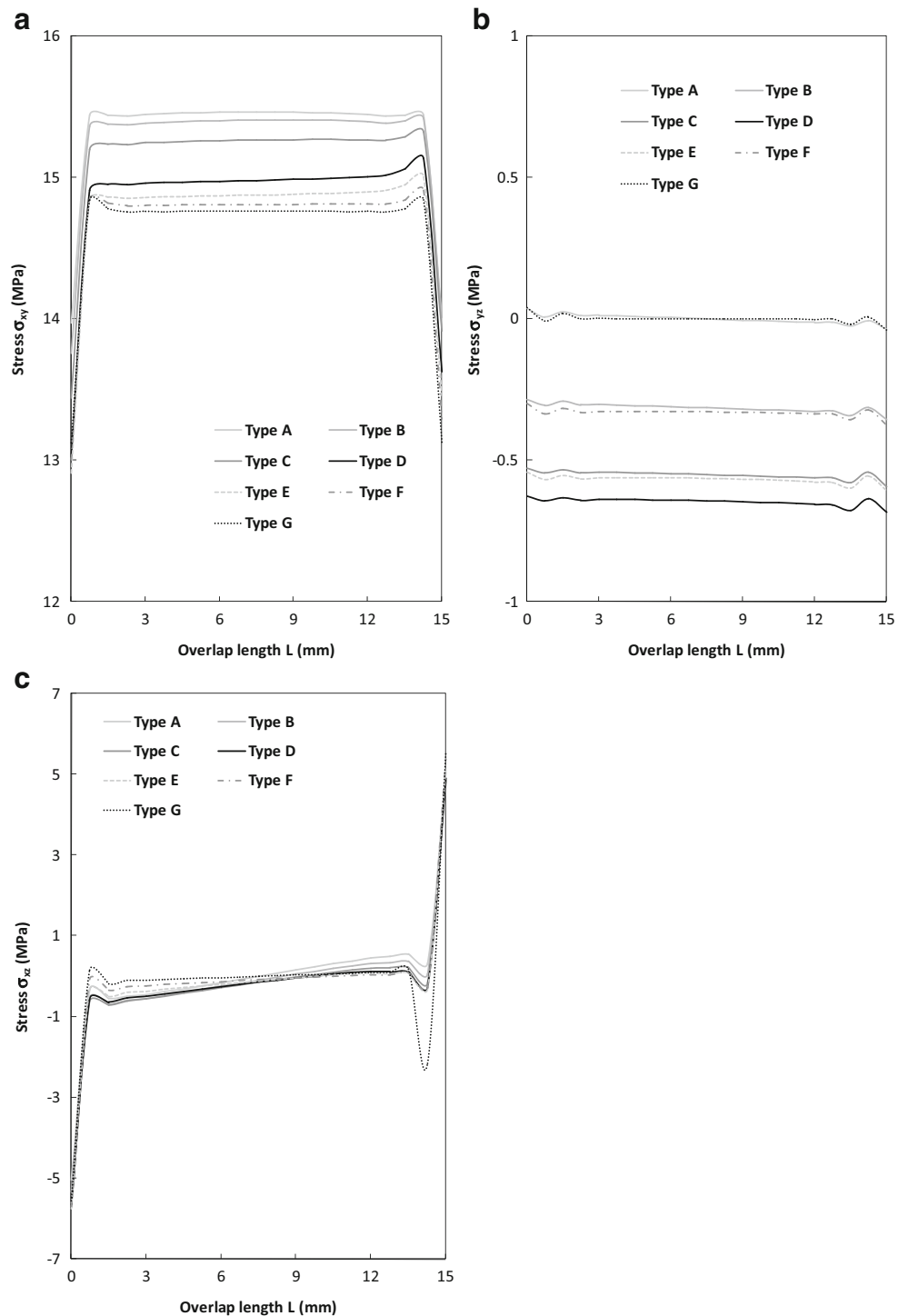

angles were jointed. The stresses were generally seen the same when composite parts with $[0°/0°/0°/0°]_s$, $[15°/−15°/15°/−15°]_s$, $[75°/−75°/75°/−75°]_s$, and $[90°/90°/90°/90°]_s$ orientation angles were jointed. In general, it was observed that σ_{xy} on adhesive layer was the biggest at $[15°/−15°/15°/−15°]_s$ orientation angles. σ_{yz}

on the adhesive layer was the biggest at $[45°/−45°/45°/−45°]_s$ orientation angles. Moreover, σ_{xz} on the adhesive layer for $[90°/90°/90°/90°]_s$ orientation angle was different than other orientation angles.

In Fig. 8, the peel and shear stresses distributions on the C-R stress line were calculated for 15 mm adherent

Fig. 8 Peel and shear stress distributions compared for Type A, Type G, and Type D along C-P on the adhesive region for 15 mm of adherent length. **a** Stress at z direction. **b** Shear stress σ_{xz}. **c** Shear stress σ_{yz}
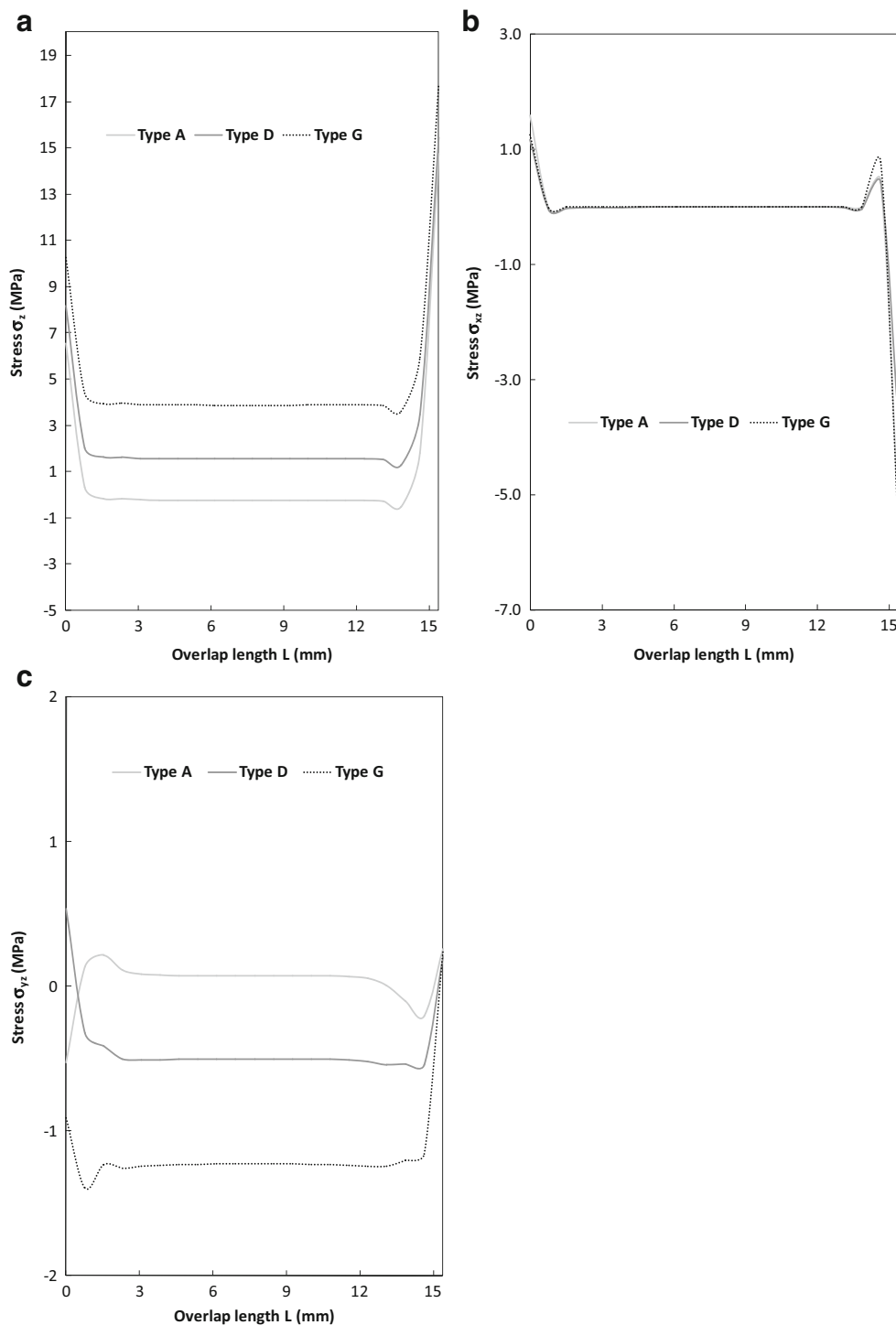
length with $[0°/0°/0°/0°]_s$, $[45°/-45°/45°/-45°]_s$ and $[90°/90°/90°/90°]_s$ orientation angles. The peel stress distribution for $[90°/90°/90°/90°]_s$ was greater than others. The σ_{xz} distribution was nearly seen the same for $[0°/0°/0°/0°]_s$, $[45°/-45°/45°/-45°]_s$, and $[90°/90°/90°/90°]_s$ orientation angles. But, the σ_{yz} distribution for $[0°/0°/0°/0°]_s$ was greater than others.

As seen in Fig. 9, the von-Mises stress distributions were calculated for different adherent length with $[0°/0°/0°/0°]_s$ orientation angles. The von-Mises stresses distribution for all adherent lengths were nearly seen the same. It could be said that the changes of adherent length and width slightly has affected the von-Mises stresses a little. In contrast to this, it could be said that they substantially changed failure loads.
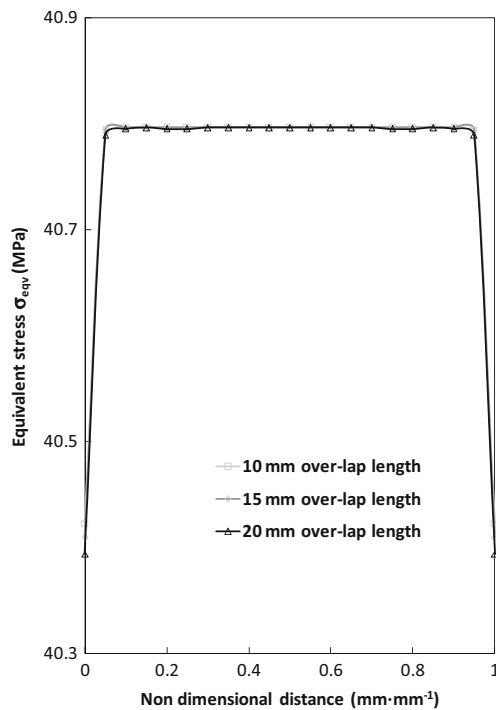
Fig. 9 The von-Mises stress distributions compared for different adherent lengths along the different bondlines (shown in Fig. 1) on the adhesive region for Type A

Table 4 Results of numerical analysis, in case of using DP 410

Specimen no.	Over-lap length L and width W (mm)	Orientation angles (°)	Failure load F (N)
1	10	Type A	6656
2		Type B	6656
3		Type C	6592
4		Type D	6528
5		Type E	6592
6		Type F	6656
7		Type G	6720
8	15	Type A	9984
9		Type B	9984
10		Type C	9984
11		Type D	9888
12		Type E	9984
13		Type F	10080
14		Type G	10080
15	20	Type A	13312
16		Type B	13312
17		Type C	13312
18		Type D	13312
19		Type E	13440
20		Type F	13440
21		Type G	13568

As a result, it could be said that $[0°/0°/0°/0°]_s$ and $[90°/90°/90°/90°]_s$ orientation angles were effective parameters for composites and joint technique. Other orientation angles are not as effective as these two orientation angles.

3.2 Effect of orientation angles and overlap on failure load

The failure loads of the composite parts bonded with the insert DLJ for different orientation angles and overlap length were given Table 4. The true tensile stress-strain behaviors for adhesives were shown in Fig. 2. In order to determine the failure load, the ultimate strain, the (ε^*) shown for the adhesive in Table 2, was used. The equivalent strain (ε_{eqv}) and stress (σ_{eqv}) were calculated using the von Misses yield criterion, and it was accepted that the failure case occurred when the equivalent strain (ε_{eqv}) calculated at any point of reached the ultimate strain for the adhesive layer. A solution in finite element analysis considering non-linear material behavior was reached by dividing the total load in steps to track the equilibrium paths and iterating to a converged solution at each load increment. Hence, a pressure of 0.5 N/mm^2 per mm^2 area at each load step was applied for all joint types and this pressure was continuous. The remaining load was then applied in the last step [24–26].

Stress at x, y, and z directions; shear stresses; and the von-Mises stresses on adhesive were calculated using numerically obtained tensile failure load. The stresses on all elements of the interfaces of composite parts and adhesive layer in Figs. 4a, b and 5, and the highest stress distributions on the joining area occurred on the S-S1stress line. That was why stresses on this line were examined during the studies.

When Table 4 and Fig. 10 were investigated, the failure loads of all the joints joined with 20 mm adherent lengths were greater than others. The predicted failure loads of composite parts with $[90°/90°/90°/90°]_s$ orientation angles were obtained as maximum at all adherent lengths. Also, the failure load of the composite parts joined with the insert DLJ with $[75°/-75°/75°/-75°]_s$ orientation angle was maximum at 15 mm overlap length. The orientation angles were important parameters for the mechanical behavior of composite laminates. It could be said that when dimensions of the adhesive region change, failure loads change.

4 Conclusions

In this work, composite parts joined with the insert DLJ subjected to tensile load were investigated by using the finite element method. The conclusions were as follows:

Fig. 10 Comparison of failure loads for all orientation angles and over lengths
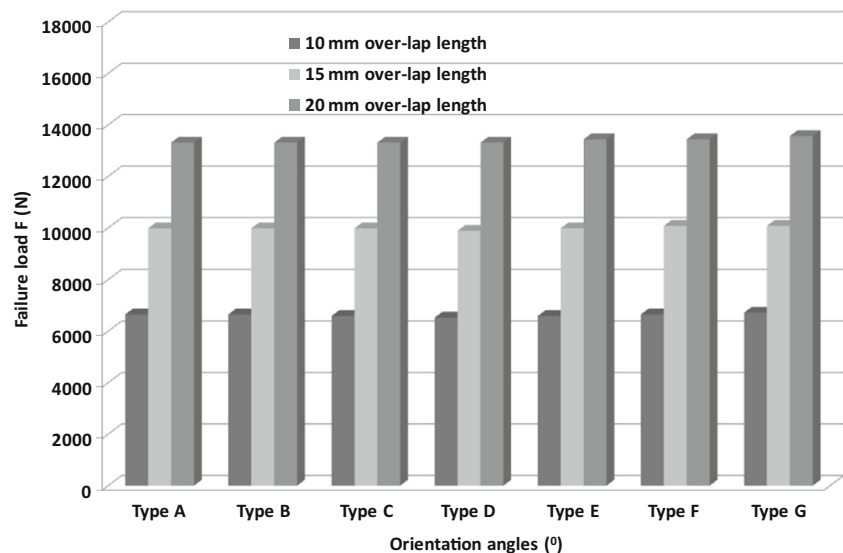
- The stresses on the S-S1 stress line were shown maximum in Fig. 5.
- The effects of different overlap lengths and different orientation angles were investigated and the failure loads of all the joints with 20-mm adherent length were greater than others were shown in Table 4 and Fig. 10.
- The maximum predicted failure loads of the joining with the insert joint were obtained, and composite parts with $[90°/90°/90°/90°]_s$ were generally higher than others were shown in Table 4 and Fig. 10.
- σ_x and σ_z on the adhesive layer were maximum when composite parts with $[90°/90°/90°/90°]_s$ orientation angles were jointed. σ_y on the adhesive layer was maximum when composite parts with $[0°/0°/0°/0°]_s$ orientation angles were jointed.
- The von Mises stress on the adhesive region was minimum when composite parts with $[45°/-45°/45°/-45°]_s$ and $[60°/-60°/60°/-60°]_s$ orientation angles were jointed. The stresses were generally seen the same when composite parts with $[0°/0°/0°/0°]_s$, $[15°/-15°/15°/-15°]_s$, $[75°/-75°/75°/-75°]_s$, and $[90°/90°/90°/90°]_s$ orientation angles were jointed.
- They were shown in Fig. 7a–c, σ_{xy} on the adhesive layer was the biggest at $[15°/-15°/15°/-15°]_s$ orientation angle. σ_{yz} on the adhesive layer was the biggest at $[45°/-45°/45°/-45°]_s$ orientation angle. Moreover, σ_{xz} on the adhesive layer for $[90°/90°/90°/90°]_s$ orientation angles was different than other orientation angles.
- In the C-R bond-line, it was shown that the peel stress distribution for $[90°/90°/90°/90°]_s$ was greater than others. The σ_{xz} distribution was nearly seen the same for $[0°/0°/0°/0°]_s$, $[45°/-45°/45°/-45°]_s$, and $[90°/90°/90°/90°]_s$ orientation angles. But, the σ_{yz}

distribution for $[0°/0°/0°/0°]_s$ was greater than others.
- The failures happened generally on the adhesive region.

References

1. Tang JH, Sridhar I, Srikanth N (2013) Static and fatigue failure analysis of adhesively bonded thick composite single lap joints. Compos Sci Technol 86:18–25. https://doi.org/10.1016/j.compscitech.2013.06.018
2. Kim KS, Yi YM, Cho GR, Kim CG (2008) Failure prediction and strength improvement of uni-directional composite single lap bonded joints. Compos Struct 82:513–520. https://doi.org/10.1016/j.compstruct.2007.02.005
3. Katnam KB, Comer AJ, Stanley WF, Buggy M, Ellingboe AR, Young TM (2011) Characterising prepreg and non-crimp-fabric composite single lap bonded joints. International Journal of Adhesion & Adhesives 31:679–686. https://doi.org/10.1016/j.ijadhadh.2011.06.013
4. Khalili SMR, Jafarkarimi MH, Abdollahi MA (2009) Creep analysis of fibre reinforced adhesives in single lap joints—experimental study. International Journal of Adhesion & Adhesives 29:656–661. https://doi.org/10.1016/j.ijadhadh.2009.02.007
5. Ariaee S, Tutunchi A, Kianvash A, Entezami AA (2014) Modeling and optimization of mechanical behavior of bonded composite–steel single lap joints by response surface methodology. International Journal of Adhesion & Adhesives 54:30–39. https://doi.org/10.1016/j.ijadhadh.2014.05.002
6. Reis PNB, Antunes FJV, Ferreira JAM (2005) Influence of super-position length on mechanical resistance of single-lap adhesive joints. Compos Struct 67:125–133. https://doi.org/10.1016/j.compstruct.2004.01.018
7. Abdi H, Papadopoulos J, Nayeb-Hashemi H, Vaziri A (2017) Enhanced elastic-foundation analysis of balanced single lap adhesive joints. International Journal of Adhesion & Adhesives 72:80–91. https://doi.org/10.1016/j.ijadhadh.2016.10.006
8. Stein N, Mardani H, Becker W (2016) An efficient analysis model for functionally graded adhesive single lap joints. International

Journal of Adhesion & Adhesives 70:117–125. https://doi.org/10.1016/j.ijadhadh.2016.06.001

9. Guin WE, Wang J (2016) Theoretical model of adhesively bonded single lap joints with functionally graded adherents. Eng Struct 124:316–332. https://doi.org/10.1016/j.engstruct.2016.06.036

10. Ribeiro TEA, Campilho RDSG, da Silva LFM, Goglio L (2016) Damage analysis of composite–aluminium adhesively-bonded single-lap joints. Compos Struct 136:25–33. https://doi.org/10.1016/j.compstruct.2015.09.054

11. Engerer JD, Sancaktar E (2011) The effects of partial bonding in load carrying capacity of single lap joints. International Journal of Adhesion & Adhesives 31:373–379. https://doi.org/10.1016/j.ijadhadh.2011.01.009

12. Tsai MY, Morton J (2010) An investigation into the stresses in double-lap adhesive joints with laminated composite adherends. Int J Solids Struct 47:3317–3325. https://doi.org/10.1016/j.ijsolstr.2010.08.011

13. Marannano G, Zuccarello B (2015) Numerical experimental analysis of hybrid double lap aluminum-CFRP joints. Compos Part B 71:28–39. https://doi.org/10.1016/j.compositesb.2014.11.025

14. Chataigner S, Caron JF, Diaz AD, Aubagnac C, Benzarti K (2010) Non-linear failure criteria for a double lap bonded joint. International Journal of Adhesion & Adhesives 30:10–20. https://doi.org/10.1016/j.ijadhadh.2009.06.007

15. Goglio L, Rossetto M (2011) Precision of the one-dimensional solutions for bonded double lap joints. International Journal of Adhesion & Adhesives 31:301–314. https://doi.org/10.1016/j.ijadhadh.2010.10.004

16. Özer H, Öz Ö (2012) Three dimensional finite element analysis of bi-adhesively bonded double lap joint. International Journal of Adhesion & Adhesives 37:50–55. https://doi.org/10.1016/j.ijadhadh.2012.01.016

17. Chuang WY, Tsai JL (2013) Investigating the performances of stepwise patched double lap joint. International Journal of Adhesion & Adhesives 42:44–50. https://doi.org/10.1016/j.ijadhadh.2013.01.005

18. Saleh P, Challita G, Khalil K (2015) Stress concentration coefficient in a composite double lap adhesively bonded joint. International Journal of Adhesion & Adhesives 63:102–107. https://doi.org/10.1016/j.ijadhadh.2015.08.005

19. Almitani KH, Othman R (2016) Analytical solution of the harmonic response of visco-elastic adhesively bonded single-lap and double-lap joints. International Journal of Adhesion & Adhesives 71:55–65. https://doi.org/10.1016/j.ijadhadh.2016.08.004

20. Liu S, Cheng X, Zhang Q, Zhang J, Bao J, Guo X (2016) An investigation of hygrothermal effects on adhesive materials and double lap shear joints of CFRP composite laminates. Composites Part B 91:431–440. https://doi.org/10.1016/j.compositesb.2016.01.051

21. Ozel A, Yazici B, Akpinar S, Aydin MD, Temiz Ş (2014) A study on the strength of adhesively bonded joints with different adherends. Compos Part B 62:167–174. https://doi.org/10.1016/j.compositesb.2014.03.001

22. Wang B, Xiong J, Wang X, Ma L, Zhang GQ, Wu LZ, Feng JC (2013) Energy absorption efficiency of carbon fiber reinforced polymer laminates under high velocity impact. Mater Des 50:140–148. https://doi.org/10.1016/j.matdes.2013.01.046

23. Sülü İY, Temiz Ş, Aydin MD (2015) Layer effects of multi-layered face to face adhesively bonded composite pipes subjected to internal pressure. Academic Journal of Science 04, No 3, pp.195–202

24. Temiz S (2006) Application of bi-adhesive in double-strap joints subjected to bending moment. J. Adhesion Sci. Technol 20, pp.1547–1560. https://doi.org/10.1163/156856106778884262

25. Sülü İsmail Yasin (2017) Mechanical behavior of internal pressurized composite pipes jointed with embedded tubular sleeves. Materials Testing 59, No. 3, 272–277. https://doi.org/10.3139/120.110996

26. Sülü İsmail Yasin (2017) Mechanical testing and analysis of composite parts adhesively joined under tensile load. Materials Testing 59(5):459–465. https://doi.org/10.3139/120.111029